Synthesis and structural characterization of 3-[1-[4-(2-methylpropyl)phenyl] ethyl]-6-(4-fluorophenyl)-1,2,4-triazolo[3,4-*b*]-1,3,4-thiadiazole

Gülsüm Gündoğdu [1,*a)] Arzu Karayel,[2] Sevim Peri Aytaç,[3] Birsen Tozkoparan,[3] and Filiz Betül Kaynak[1]
[1]*Faculty of Engineering, Department of Physics Engineering, Hacettepe University, 06800 Beytepe, Ankara, Turkey*
[2]*Faculty of Arts and Sciences, Department of Physics, Hitit University, 19030 Çorum, Turkey*
[3]*Faculty of Pharmacy, Department of Pharmaceutical Chemistry, Hacettepe University, 06100 Sıhhiye, Ankara, Turkey*

(Received 3 April 2019; accepted 21 July 2019)

3-[1-[4-(2-Methylpropyl)phenyl]ethyl]-6-(4-fluorophenyl)-1,2,4-triazolo[3,4-*b*]-1,3,4-thiadiazole ($C_{21}H_{21}FN_4S$) has been synthesized as a member of a series of triazolothiadiazoles having NSAIDs moieties with cytotoxic activity. The crystal structure of this new compound has been solved and refined using conventional laboratory X-ray powder diffraction data and optimized using density functional techniques. The final structure solution was achieved by Rietveld refinement using soft restraints on all non-H atom bond lengths and angles. This compound crystallizes in $P\bar{1}$ space group, with the unit cell parameters $a = 5.5880(4)$ Å, $b = 9.3074(7)$ Å, $c = 19.497(4)$ Å, $\alpha = 99.311(10)°$, $\beta = 91.925(9)°$, $\gamma = 98.199(6)°$, and $V = 988.8(2)$ Å^3. To complement and verify the structure solution of the compound, the density functional theory (DFT) calculations were performed by using the local density approximation and the generalized gradient approximation for exchange-correlation energy. In order to see the effect of the van der Waals interactions on the electronic structure, the relevant structure was also optimized with B3LYP-D2, PBE-D2, and optB88-vdW functionals. The refined crystal structure was confirmed by the DFT calculations. The best agreement with the experimental structure was achieved by optB88-vdW functional. © *2019 International Centre for Diffraction Data*. [doi:10.1017/S0885715619000654]

Key words: 1,2,4-triazolo[3,4-*b*]-1,3,4-thiadiazole derivatives, laboratory X-ray powder diffraction, Rietveld refinement, crystal structure, DFT

I. INTRODUCTION

Throughout the past ten years, a great deal of condensed aminomercaptotriazole derivatives with analgesic/anti-inflammatory and cytotoxic activity have been synthesized (Aytaç *et al*., 2009, 2016; Tozkoparan *et al*., 2009, 2012). In a previous work (Aytaç *et al*., 2016) reported that a series of triazolothiadiazines, display significant *in vitro* cytotoxic activity on human epithelial cancers, especially liver cancer. In order to add new members to this promising chemical series, new analog compounds, named 1,2,4-triazolo [3,4-*b*]-1,3,4-thiadiazole, have been prepared by bioisosteric replacement of the triazolothiadiazine ring with a triazolothiadiazole one. The compound is one example of this series having a cytotoxic activity which is obtained as powder. The crystal structure determination of the compound was accomplished by X-ray powder diffraction (PXRD).

We introduce here, the preparation and structural characterization of 3-[1-[4-(2-methylpropyl)phenyl]ethyl]-6-(4-fluorophenyl)-1,2,4-triazolo[3,4-*b*]-1,3,4-thiadiazole, as well as structure solution by laboratory X-ray powder diffraction data (PXRD) supported by the density functional theory (DFT) calculations. We performed a comprehensive first principles study on the structural properties of the compound. Structure optimization calculations were completed with both pure DFT and dispersion-corrected density functional theory (DFT-D). It is important to consider the van der Waals effects for molecular crystal structures, therefore optB88-vdW, B3LYP-D2, and PBE-D2 functionals were realized. Finally, the geometric parameters of the crystal structure obtained by Rietveld refinement were compared with the optimized structures.

II. EXPERIMENTAL

A. Instrumentation

Melting heat was determined on a Thomas Hoover capillary melting point apparatus (Philadelphia, PA, USA) and was uncorrected. IR spectra were recorded on a Perkin Elmer 1720X FT-IR spectrometer (Beaconsfield, UK) by direct sampling of the compounds. ^{1}H-NMR spectra were recorded on a Varian Mercury 400, a 400-MHz High-Performance Digital FT-NMR instrument (Varian, Palo Alto, CA, USA) in $CDCl_3$ using tetramethylsilane as an internal standard. High-Resolution Mass Spectra (HRMS) data were collected with a Waters Micromass ZQ LC-MS Spectrometer (Milford, MA, USA) instrument using the ESI (+) method. Elementary analysis of the resulting compound was performed with Leco CHNS 932 analyzer at Ankara University, Faculty of Pharmacy Central II Laboratory and data were determined within ±0.4% of the theoretical values.

* This article is a part of the PhD thesis of Gülsüm Gündoğdu.
[a)]Author to whom correspondence should be addressed. Electronic mail: gulsum.gnd@hacettepe.edu.tr

B. Synthesis of the compounds

The preparation of the title compound was carried out in two steps (Figure 1). Firstly, commercially available ibuprofen reacted with thiocarbohydrazide at its melting point (about 170 °C) to obtain aminomercaptoriazole derivative (Aytaç *et al.*, 2016). In the second step, the reaction of aminomercaptoriazole scaffold with 4-fluoro benzoic acid in phosphorus oxychloride via a one-pot two-component reaction gave target compound (Tozkoparan *et al.*, 2012). The structure of the new compound was fully established by IR, ^{1}H-NMR, mass spectrometry, and elemental analysis. All data of the compound were in full agreement with the proposed structure.

3-[1-[4-(2-Methylpropyl)phenyl]ethyl]-6-(4-fluorophenyl)-1,2,4-triazolo[3,4-b]-1,3,4-thiadiazole

0.20 g (52.57%). M.p.: 151–152 °C. IR: *ν*max: 1601 (C=N), 1308 (C–N) cm^{-1}; ^{1}H-NMR ($CDCl_3$) δ (ppm) 0.87 (6H, *d*, $(CH_3)_2$–CH–), 1.80–1.84 (1H, *m*, $(CH_3)_2$–C*H*–CH_2–), 1.91 (3H, *d*, CH_3–CH–), 2.43 (2H, *d*, –CH–CH_2–), 4,65 (1H, *q*, CH_3–C*H*–), 7.10 (2H, *d*, arom. H), 7.20 (2H, *t*, arom. H), 7.34 (2H, *d*, arom. H), 7.79–7.83 (2H, *m*, arom. H); MS (ESI+) *m/z* Calcd. for $C_{21}H_{22}FN_4S$ $(M+H)^+$ 381.15, found 381.13; Anal. Calcd. for $C_{21}H_{21}FN_4S$: C, 66.29; H, 5.56; N, 14.73; S, 8.43. Found: C, 66.57; H, 5.72; N, 14.86; S, 8.57.

C. PXRD data collection

PXRD of the compound was collected in Debye–Scherrer type geometry using Bruker D8 Advance powder diffractometer operated at 48 kV, 38 mA with molybdenum radiation ($\lambda_{K\alpha1}$ = 0.709 Å, $\lambda_{K\alpha2}$ = 0.71 Å) and equipped with a Göbel-mirror on the primary side monochromator and a position sensitive silicon-strip detector named "Lynx-Eye". The following optics were used: primary beam soller slit (0.4 mm), divergence slit (0.4 mm), and receiving soller slit (1.5°). The powder sample of the compound loaded in a 0.7-mm diameter glass capillary after griding using a mortar. The diffracted intensities were collected at room temperature (295.0 K) in the range from 0° to 40° (2θ) in step-scan mode with a step size of 0.008° and a counting time of 15 s/step.

D. PXRD data analysis

Indexing of the PXRD pattern was carried out using the TOPAS Academic program v5.1 (Coelho, 2012), yielding the following values for triclinic space group $P\bar{1}$ of the compound: a = 5.576 Å, b = 9.281 Å, c = 19.486 Å, α = 99.33°, β = 91.95°, γ = 98.18°, V = 983.30 Å^3, and GOF = 15.14.

Then, Pawley refinement for the whole powder pattern of the compound was performed to confirm the choice of space group as well as the unit cell parameters. The unit cell parameters, *R*-factors and goodness-of-fit indicator were obtained as a = 5.5866(6) Å, b = 9.300(1) Å, c = 19.470(7) Å, α = 99.259 (15)°, β = 92.001(15)°, γ = 98.159(11)° and V = 986.6(4) Å^3, R_{wp} = 3.034%, R_{exp} = 1.078% and χ^2 = 2.814 with a good visual fit of the whole pattern. PXRD of the compound is given in Supplementary Table S1. The d_{obs} values in the table are taken directly from the PXRD. The peak that has the strongest intensity in the entire pattern is assigned of 100 and other lines are scaled relative to this value for the data set.

A template of the molecule was built and full geometry optimization at DFT/B3LYP level using the 6–31G++(*d*,*p*) basis set was performed with Gaussian 09 program (Frisch *et al.*, 2009). The molecule without hydrogen atoms was used as a fragment to solve the initial structure with the Monte Carlo simulated annealing (parallel tempering algorithm) method implemented in FOX program (Favre-Nicolin and Černý, 2002). During the simulated annealing calculations, global parameters defining the orientation and the position of each fragment are varied during the procedure, together with torsion angles. The best solution with 62 788.61 overall best cost was obtained.

Having obtained the initial structure and profile terms, the Rietveld refinement in 2θ range from 1° to 35° was carried out using TOPAS Academic program v5.1. The background was fitted using 5-order Chebyshev polynomials. The peak asymmetry was fitted by the simple axial divergence model of Cheary and Coelho (1998). The peak profiles modeled by the Double-Voigt approach (Balzar, 1993; Coelho, 2012). During the refinement, unit-cell parameters, background, zero-point error, scale factor, peak width, and asymmetry parameters were refined together with non-H atomic coordinates. Soft restraints to all non-H atom bond lengths and angles, as well as soft planar group restraints to all rings, were applied. The values used in the soft restraints on the bond lengths and angles were taken from the optimized structure with local density approximation (LDA) functional (van de Streek, 2015).

Afterwards, the coordinates of the S and F atoms were refined one by one. The atoms of each ring were refined together followed by one ring after another. For all non-H atoms, an overall isotropic atomic displacement parameter (B_{iso}) was determined and refined. Before the final refinement, the hydrogen atoms were introduced from geometrical

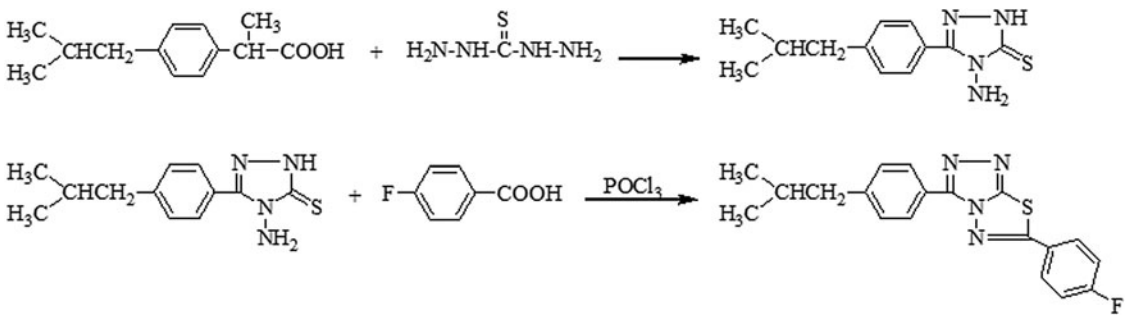

Figure 1. The synthesis scheme of the compound.

https://doi.org/10.1017/S0885715619000654 Published online by Cambridge University Press

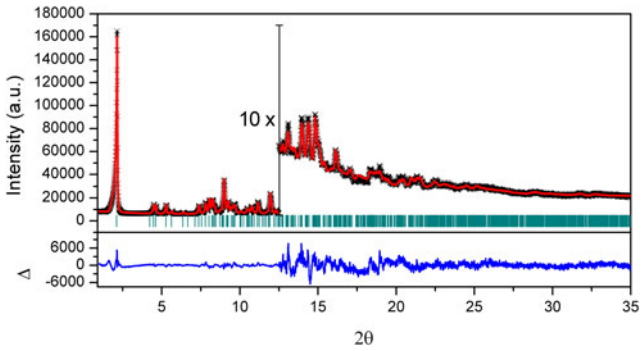

Figure 2. Plot of the final Rietveld refinement of the compound. Black crosses represent the observed data, the red line indicates the calculated pattern, and the blue line at the bottom represents the difference between the observed and calculated patterns. Green vertical bars indicate Bragg reflections.

arguments (C–H = 0.96 Å and B_{iso} (H) = 1.2 B_{iso} (C)) by using Crystals program (Cooper *et al.*, 2010). The fractional coordinates of the hydrogen atoms were refined by riding motion approximation with a macro implemented in TOPAS. Their isotropic atomic displacements (B_{iso}) were constrained to be 1.2 times the value of the carrier atom. The Rietveld refinement was converged with a smooth difference curve (Figure 2). The structure refinement details are summarized in Table I.

E. Computational methods

The correctness of the experimental crystal structures has been validated previously for 241 organic compounds, which shows that DFT calculations are an effective tool for the reproduction of molecular structures (van de Streek and Neumann, 2010). Due to the relatively low amount of powder XRD data (with an upper 2θ limit of 35°), it was aimed to perform DFT calculations in order to complement and verify the experimental structure solution of the compound.

In the theoretical calculations, the crystal structure was modeled using the first principles calculations based on DFT as performed in Vienna *ab initio* simulation package (VASP) (Kresse and Hafner, 1993; Kresse and Furthmüller, 1996a, 1996b). Starting from the experimental structure solution, the crystal structure optimizations were carried out with fixed unit cell parameters. The electron–ion interactions were described by projector augmented waves (PAW) (Blöchl, 1994; Kresse and Joubert, 1999) with plane-waves up to the energy of 800 eV. The effects of exchange-correlations were examined by using the LDA (CA-PZ) (Ceperley and Alder, 1980; Perdew and Zunger, 1981) and the generalized gradient approximation (GGA) in the parametrization of Perdew–Burke–Ernzerhof (PBE) (Perdew *et al.*, 1996) functional. In addition to these functionals, the van der Waals (vdW) functional (optB88-vdW) (Klimeš *et al.*, 2010) was also utilized. By using the optB88-vdW functional, the PBE functional was modified to generate the PAW core potentials. Additionally, DFT-D2 developed by Grimme (2006) was also used. Brillouin zone is sampled with 5 × 3 × 1 Monkhorst–Pack (Monkhorst and Pack, 1976). The relaxations of all structures were performed by using the conjugate gradient method. The total energies of all atoms in the system were converged to 10^{-6} eV atom^{-1}. The energy values of the optimized structures of the compound were given in Table II.

TABLE I. Crystal data and structure refinement parameters of the compound.

Crystal data	
Chemical formula	$C_{21}H_{21}FN_4S$
M_r	380.48
Crystal system, space group	Triclinic, $P\bar{1}$
Temperature (K)	295
a, b, c (Å)	5.5880(4), 9.3074(7), 19.497(4)
α, β, γ (°)	99.311(10), 91.925(9), 98.199(6)
V (Å^3)	988.8(2)
Z	2
Radiation type	Mo $K\alpha$, λ = Mo $K\alpha1$ = 0.70926 Å, $K\alpha2$ = 0.71354 Å
μ (mm^{-1})	0.19
Specimen shape, size (mm)	Cylinder, 10 × 0.7 mm
Data collection	
Diffractometer	Bruker D8 Advance
Specimen mounting	Glass capillary
Data collection mode	Transmission
Scan method	Step
2θ values (°)	$2\theta_{min}$ = 1, $2\theta_{max}$ = 35, $2\theta_{step}$ = 0.008
Refinement	
R-factors and goodness-of-fit	R_p = 2.762%, R_{wp} = 3.537%, R_{exp} = 1.284%, R_{Bragg} = 1.278%, χ^2 = 2.754
d-DW	0.2838
No. of data points	4248
No. of parameters	103
No. of restraints	66
H-atom treatment	H-atom parameters constrained

III. RESULTS AND DISCUSSION

The Rietveld refined and the DFT-optimized structures are overlaid for the comparison shown in Figure 3. The root-mean-square (r.m.s.) differences between the coordinates of the Rietveld refined and the DFT-optimized structures for the non-H atoms are 0.219 Å with LDA, 0.181 Å with PBE, 0.188 Å with B3LYP-D2, 0.189 Å with PBE-D2, and 0.177 Å with optB88-vdW functional, which are in the range expected for correct powder structures obtained from the laboratory PXRD [Note: It should be below 0.25 Å (van de Streek and Neumann, 2014)]. The conservation of the packing arrangement and the good agreement between the refined and the optimized structures of the compound supports the validity of our structure solution (van de Streek and Neumann, 2014).

Long-range dispersive interactions (van der Waals interactions) are particularly important for prediction of the organic crystal structures. Even though the pure DFT calculations could give good results, it is limited to describe correctly van der Waals interactions. Since an accurate description of dispersion interactions provide an advantage, DFT calculations with van der Waals corrections and functional were

TABLE II. Energy values of the optimized structures of the compound.

LDA	E_0 = −659.94734 eV
PBE-D2	E_0 = −618.84443 eV
B3LYP-D2	E_0 = −618.84337 eV
PBE	E_0 = −613.01133 eV
optB88-vdW	E_0 = −541.85408 eV

https://doi.org/10.1017/S0885715619000654 Published online by Cambridge University Press

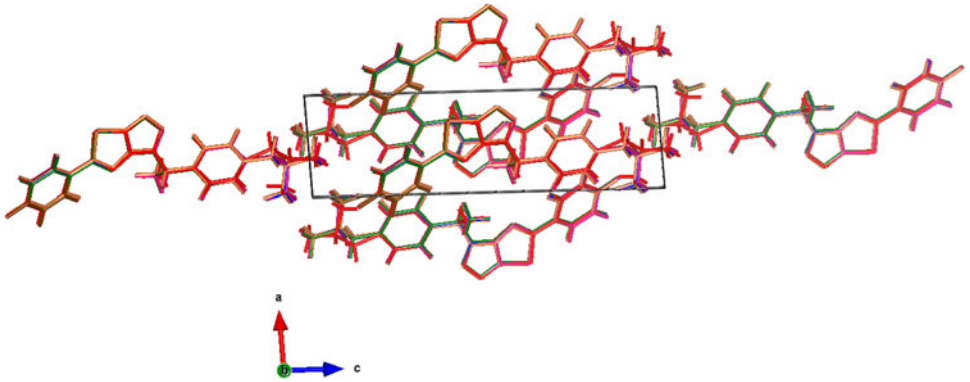

Figure 3. Comparison of the experimental crystal structure from powder data (red) and the calculated structure by DFT investigations with LDA (orange), optB88-vdW (brown), PBE (pink), B3LYP-D2 (blue), and PBE-D2 (green) functionals projected onto *ac* plane.

performed. In the literature, it is not observed previously that the structure solution obtained from laboratory PXRD was supported by the optB88-vdW functional. A large number of experimental organic crystal structures were verified by using the DFT-D method (van de Streek and Neumann, 2010). In our study, the experimental structure was compared with the optimized structures obtained with the pure DFT, DFT-D2, and optB88-vdW functionals. The best match was gained from the optimization with optB88-vdW functional.

The bond lengths and angles within the triazolo-thiadiazole system of the refined structure agreed well with the reference structures (Lu *et al*., 2008; Khan *et al*., 2009, 2014; Fan *et al*., 2010; Cansız *et al*., 2012; Wu, 2013; Gündoğdu *et al*., 2017) and the optimized structures (Table III). The Ortep-3 (Farrugia, 2012) diagram of the compound with thermal ellipsoids at the 50% probability level is shown in Figure 4.

In the discussion part of the geometry, the DFT optimized structure with optB88-vdW functional was used, because the hydrogen bonds (Table IV) are analyzed better in the optimized structures (Kaduk *et al*., 2016). As expected, the 1,2,4-triazolo, 1,3,4-thiadiazole, and phenyl rings are essentially planar. The highest deviations from the planarity are 0.001 Å, 0.004 Å, 0.005 Å, and 0.008 Å, respectively for the 1,2,4-triazolo ring, the 1,3,4-thiadiazole ring, the C16–C21 ring, and the C5–C10 ring. An intermolecular C17–H171···S1 interaction supports the planarity of the molecular structure.

The 1,2,4-triazolo ring is almost coplanar with the 1,3,4-thiadiazole ring with a mean deviation of 0.005 Å, which forms a dihedral angle of 0.53°. The dihedral angles

TABLE III. Selected bond lengths and angles (Å, °) for the experimental (PXRD) and optimized structures of the compound.

Parameter	PXRD	LDA	PBE	B3LYP-D2	PBE-D2	optB88-vdW
N1–C13	1.32(8)	1.3192	1.3261	1.3269	1.3271	1.3261
N1–N2	1.36(8)	1.3728	1.3930	1.3930	1.3930	1.3945
N2–C14	1.32(9)	1.3127	1.3196	1.3203	1.3205	1.3195
N3–C14	1.36(10)	1.3673	1.3784	1.3789	1.3791	1.3775
N3–C13	1.36(11)	1.3622	1.3778	1.3742	1.3738	1.3787
N3–N4	1.34(8)	1.3429	1.3632	1.3615	1.3615	1.3633
N4–C15	1.35(10)	1.3054	1.3152	1.3152	1.3151	1.3128
S1–C15	1.72(6)	1.7129	1.7724	1.7259	1.7737	1.7269
S1–C14	1.77(8)	1.7621	1.7250	1.7750	1.7257	1.7823
F1–C19	1.35(7)	1.3466	1.3650	1.3660	1.3659	1.3662
N1–C13–N3	107(6)	107.46	107.73	107.76	107.80	107.61
N2–N1–C13	110(6)	109.87	109.90	109.86	109.87	109.79
N1–N2–C14	106(5)	106.19	105.66	105.66	105.61	105.90
N2–C14–N3	110(7)	109.93	110.72	110.61	110.66	110.44
C14–N3–C13	107(6)	106.53	105.97	106.11	106.06	106.26
S1–C14–N3	109(5)	109.33	109.32	109.14	109.05	109.38
C15–S1–C14	87(4)	87.58	87.86	87.85	87.93	87.80
S1–C15–N4	117(5)	116.30	116.36	116.37	116.34	115.98
N3–N4–C15	108(5)	108.07	107.97	107.83	107.84	108.34
C14–N3–N4	119(6)	118.72	118.49	118.80	135.11	118.48
C18–C19–F1	120(6)	118.74	118.80	118.67	118.67	118.57
C20–C19–F1	121(5)	118.68	118.67	118.67	118.64	118.62
N3–N4–C15–C16	−174(6)	−179.78	−177.87	−179.15	−179.08	−178.35
C12–C11–C13–N3	81(7)	70.85	68.18	70.99	70.98	69.32
C7–C8–C11–C12	−130(6)	−119.95	−124.57	−125.36	−125.64	−125.70
C3–C4–C5–C6	92(9)	101.40	103.73	100.85	101.21	103.63
C1–C3–C4–C5	−142(5)	173.12	172.90	174.08	173.66	174.45
C2–C3–C4–C5	−21(7)	−63.17	−63.52	−62.67	−63.05	−62.10

https://doi.org/10.1017/S0885715619000654 Published online by Cambridge University Press

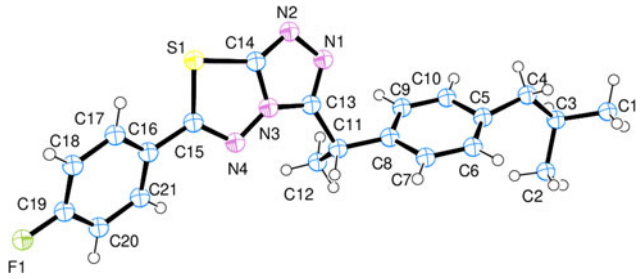

Figure 4. View of the title molecule showing the atomic numbering and 50% probability displacement spheres.

between the triazole-thiadiazole ring system and the planes of the C16–C2 and the C5–C10 rings are 19.72° and 66.36°, respectively.

There are two C–H···π intermolecular hydrogen-bonding interactions. The first of them is between the atom H123 and the centroid of the 1,3,4-thiadiazole ring with a distance of 2.71 Å (symmetry code: $1-x,1-y,1-z$) and the centroid angle is 129° (Supplementary Figure S1). The second one is between the atom H171 and the centroid of the C5–C10 ring and the distance is 2.80 Å (symmetry code: $1-x, 2-y, 1-z$) and the centroid angle is 140° (Supplementary Figure S2). There is a chiral center at C11 atom in the structure.

The first short intermolecular contact of the triazolothiadiazole ring containing structures in the literature was observed in the study of Khan *et al.* (2015) as 2.795(2) Å, which is shorter than the van der Waals radii sum of nitrogen and sulfur atoms (3.35 Å) for S···N. The short intermolecular contact is also found in the title structure (between the symmetry codes: x, y, z and $2-x$, $2-y$, $1-z$) for S1···N2 with 2.96 Å.

In addition, weak π–π stacking interactions between the 1,3,4-thiadiazole ring and 1,2,4-triazolo ring (between symmetry codes: x, y, z and $1-x$, $2-y$, $1-z$) with a centroid–centroid distance of 3.4345 Å is observed. The two

TABLE IV. Hydrogen bonding geometry (Å, °) for the experimental (PXRD) and optimized structures of the compound.

	D–H···A	D–H	H···A	D···A	D–H···A
PXRD	C17–H171···S1	0.95	2.65	3.08	108
LDA	C7–H71···N1^{i}	1.10	2.32	3.388	162
	C11–H111···N2^{i}	1.11	2.57	3.651	163
	C12–H123···N4^{ii}	1.10	2.58	3.5582	147
	C17–H171···S1	1.10	2.71	3.1252	102
PBE	C7–H71···N1^{i}	1.09	2.47	3.50	157
	C11–H111···N2^{i}	1.10	2.55	3.615	162
	C12–H123···N4^{ii}	1.10	2.62	3.6080	149
	C17–H171···S1	1.09	2.71	3.1382	103
B3LYP-D2	C7–H71···N1^{i}	1.09	2.43	3.4674	159
	C11–H111···N2^{i}	1.10	2.59	3.6472	160
	C12–H123···N3^{ii}	1.10	2.61	3.2933	119
	C12–H123···N4^{ii}	1.10	2.61	3.5955	150
	C17–H171···S1	1.09	2.76	3.1607	101
PBE-D2	C7–H71···N1^{i}	1.09	2.43	3.4726	159
	C11–H111···N2^{i}	1.10	2.59	3.6473	160
	C12–H123···N3^{ii}	1.10	2.61	3.2939	120
	C12–H123···N4^{ii}	1.10	2.61	3.6043	150
	C17–H171···S1	1.09	2.76	3.1601	101
optB88-vdW	C7–H71···N1^{i}	1.10	2.45	3.4911	158
	C11–H111···N2^{i}	1.11	2.59	3.6470	160
	C17–H171···S1	1.09	2.72	3.1427	103

Symmetry codes: (i) $x-1$, y, z; (ii) $-x+1$, $-y+1$, $-z+1$.

C–Hπ interactions, short intermolecular contacts (S···N and C···N), π–π stacking interactions and inter molecular hydrogen bonds (Table IV) link the molecules into a three-dimensional network (Supplementary Figure S3).

IV. CONCLUSION

The preparation of the originally synthesized compound, structural characterization and its crystal structure achieved from the PXRD are reported in this study, which is consistent with the DFT calculations. When compared both pure DFT and DFT-D results, the best agreement with the refined structure was achieved by optB88-vdW functional. To the best of our knowledge, there is no study before by validation with optB88-vdW functional of the experimental structure solution obtained from the PXRD. The good agreement between the refined and optimized structures (Figure 3) is the strong evidence that the structure is correct.

SUPPLEMENTARY MATERIAL

The supplementary material for this article can be found at https://doi.org/10.1017/S0885715619000654.

ACKNOWLEDGMENTS

Financial support to Gülsüm Gündoğdu from The Scientific and Technological Research Council of Turkey (TÜBİTAK) is gratefully acknowledged (2214-A one-year international research grant during PhD). She is indebted to Professor Hermann Gies and his work group for Crystal Chemistry from the Ruhr University Bochum, Institute for Geology, Mineralogy and Geophysics, Department of Crystallography, for hosting her during the period of one year. The authors thank also to Hacettepe University Research Center to purchase the TOPAS Academic program (Project ID: 9460, FHD-2016-9460). The numerical calculations reported in this paper were fully performed at TUBITAK ULAKBIM, High Performance and Grid Computing Center (TRUBA resources).

Aytaç, S. P., Tozkoparan, B., Kaynak, F. B., Aktay, G., Göktaş, Ö., and Ünüvar, S. (**2009**). "Synthesis of 3,6-disubstituted 7H-1,2,4-triazolo [3,4-*b*]-1,3,4-thiadiazines as novel analgesic/anti-inflammatory compounds," Eur. J. Med. Chem. **44**(11), 4528–4538.

Aytaç, P. S., Durmaz, I., Houston, D. R., Çetin-Atalay, R., and Tozkoparan, B. (**2016**). "Novel triazolothiadiazines act as potent anticancer agents in liver cancer cells through Akt and ASK-1 proteins," Bioorg. Med. Chem. **24**(4), 858–872.

Balzar, D. (**1993**). "X-ray diffraction line broadening: modeling and applications to high-Tc superconductors," J. Res. Natl. Inst. Stand. Technol. **98**(3), 321–353.

Blöchl, P. E. (**1994**). "Projector augmented-wave method," Phys. Rev. B. **50**(24), 17953–17979.

Cansız, A., Cetin, A., Orek, C., Karatepe, M., Sarac, K., Kus, A., and Koparir, P. (**2012**). "6-Phenyl-3-(4-pyridyl)-1,2,4-triazolo-[3,4-*b*][1,3,4]thiadiazole: synthesis, experimental, theoretical characterization and biological activities," Spectrochim. Acta A Mol. Biomol. Spectrosc. **97**, 606–615.

Ceperley, D. M. and Alder, B. J. (**1980**). "Ground state of the electron gas by a stochastic method," Phys. Rev. Lett. **45**(7), 566–569.

Cheary, R. W. and Coelho, A. A. (**1998**). "Axial divergence in a conventional X-ray powder diffractometer. I. Theoretical foundations," J. Appl. Crystallogr. **31**(6), 851–861.

Coelho, A. A. (**2012**). *TOPAS Academic Version 5: User Manual.*

Cooper, R. I., Thompson, A. L., and Watkin, D. J. (**2010**). "CRYSTALS enhancements: dealing with hydrogen atoms in refinement," J. Appl. Crystallogr. **43**(5 Pt 1), 1100–1107.

Fan, Z., Yang, Z., Zhang, H., Mi, N., Wang, H., Cai, F., Zuo, X., Zheng, Q., and Song, H. (**2010**). "Synthesis, crystal structure, and biological activity of 4-methyl-1,2,3-thiadiazole-containing 1,2,4-triazolo[3,4-*b*][1,3,4]thiadiazoles," J. Agric. Food. Chem. **58**(5), 2630–2636.

Farrugia, L. J. (**2012**). "WinGX and ORTEP for windows: an update," J. Appl. Crystallogr. **45**(4), 849–854.

Favre-Nicolin, V. and Černý, R. (**2002**). "FOX, 'free objects for crystallography': a modular approach to *ab initio* structure determination from powder diffraction," J. Appl. Crystallogr. **35**(6), 734–743.

Frisch, M. J., Trucks, G. W., Schlegel, H. B., Scuseria, G. E., Robb, M. A., Cheeseman, J. R., Scalmani, G., Barone, V., Mennucci, B., Petersson, G. A., Nakatsuji, H., Caricato, M., Li, X., Hratchian, H. P., Izmaylov, A. F., Bloino, J., Zheng, G., Sonnenberg, J. L., Hada, M., Ehara, M., Toyota, K., Fukuda, R., Hasegawa, J., Ishida, M., Nakajima, T., Honda, Y., Kitao, O., Nakai, H., Vreven, T., Montgomery Jr., J. A., Peralta, J. E., Ogliaro, F., Bearpark, M., Heyd, J. J., Brothers, E., Kudin, K. N., Staroverov, V. N., Kobayashi, R., Normand, J., Raghavachari, K., Rendell, A., Burant, J. C., Iyengar, S. S., Tomasi, J., Cossi, M., Rega, N., Millam, J. M., Klene, M., Knox, J. E., and Cross, J. B. (**2009**). *GAUSSIAN 09 (Revision A.1)* (Gaussian, Inc., Wallingford, CT).

Grimme, S. (**2006**). "Semiempirical GGA-type density functional constructed with a long-range dispersion correction," J. Comput. Chem. **27**(15), 1787–1799.

Gündoğdu, G., Aytaç, S. P., Müller, M., Tozkoparan, B., and Kaynak, F. B. (**2017**). "Structure determination of two structural analogs, named 3-[1-(2-fluoro-4-biphenyl)ethyl]-6-(4-fluorophenyl)-1,2,4-triazolo[3,4-*b*]-1,3,4-thiadiazole ($C_{23}H_{16}F_2N_4S$) and 3-[1-(2-fluoro-4-biphenyl)ethyl]-6-(4-chlorophenyl)-1,2,4-triazolo[3,4-*b*]-1,3,4-thiadiazole ($C_{23}H_{16}ClFN_4S$) by synchrotron X-ray powder diffraction," Powder Diffr. **32**(4), 279–289.

Kaduk, J. A., Gindhart, A. M., and Blanton, T. N. (**2016**). "Crystal structure of norgestimate, $C_{23}H_{31}NO_3$," Powder Diffr. **31**(4), 274–278.

Khan, M. H., Hameed, S., Tahir, M. N., Bokhari, T. H., and Khan, I. U. (**2009**). "6-(1-Adamantyl)-3-(2-fluorophenyl)-1,2,4-triazolo[3,4-*b*][1,3,4] thiadiazole," Acta Crystallogr. E. **65**, o1437.

Khan, I., Zaib, S., Ibrar, A., Rama, N. H., Simpson, J., and Iqbal, J. (**2014**). "Synthesis, crystal structure and biological evaluation of some novel 1,2,4-triazolo[3,4-*b*]-1,3,4-thiadiazoles and 1,2,4-triazolo[3,4-*b*]-1,3,4-thiadiazines," Eur. J. Med. Chem. **78**, 167–177.

Khan, I., Bakht, S. M., Ibrar, A., Abbas, S., Hameed, S., White, J. M., Rana, U. A., Zaib, S., Shahid, M., and Iqbal, J. (**2015**). "Exploration of a library of triazolothiadiazole and triazolothiadiazine compounds as a highly potent and selective family of cholinesterase and monoamine oxidase inhibitors: design, synthesis, X-ray diffraction analysis and molecular docking studies," RSC Adv. **5**(27), 21249–21267.

Klimeš, J., Bowler, D. R., and Michaelides, A. (**2010**). "Chemical accuracy for the van der Waals density functional," J. Phys. Condens. Matter **22**, 022201.

Kresse, G. and Furthmüller, J. (**1996a**). "Efficient iterative schemes for *ab initio* total-energy calculations using a plane-wave basis set," Phys. Rev. B. **54**, 11169–11186.

Kresse, G. and Furthmüller, J. (**1996b**). "Efficiency of ab-initio total energy calculations for metals and semiconductors using a plane-wave basis set," Comput. Mater. Sci. **6**, 15–50.

Kresse, G. and Hafner, J. (**1993**). "*Ab initio* molecular dynamics for liquid metals," Phys. Rev. B. **47**, 558–561.

Kresse, G. and Joubert, D. (**1999**). "From ultrasoft pseudopotentials to the projector augmented-wave method," Phys. Rev. B. **59**, 1758–1775.

Lu, D., Zhang, M., Song, L., Tan, Q., and Shao, M. (**2008**). "Ethyl 5-[6-(furan-2-yl)-1,2,4-triazolo[3,4-*b*][1,3,4]thiadiazol-3-yl]-2,6-dimethylnicotinate," Acta Crystallogr. E. **64**, o80–o81.

Monkhorst, H. J. and Pack, J. D. (**1976**). "Special points for Brillouin-zone integrations," Phys. Rev. B. **13**(12), 5188.

Perdew, J. P. and Zunger, A. (**1981**). "Self-interaction correction to density-functional approximations for many-electron systems," Phys. Rev. B. **23**, 5048–5079.

Perdew, J. P., Burke, K., and Ernzerhof, M. (**1996**). "Generalized gradient approximation made simple," Phys. Rev. Lett. **77**, 3865–3868.

Tozkoparan, B., Aytaç, S. P., and Aktay, G. (**2009**). "Novel 3,6-disubstituted 7H-1,2,4-triazolo[3,4-*b*][1,3,4]thiadiazines: synthesis, characterization, and evaluation of analgesic/anti-inflammatory, antioxidant activities," Arch. Pharm. Chem. Life Sci. **342**, 291–298.

Tozkoparan, B., Aytac, P. S., Gursoy, S., Gunal, S., and Aktay, G. (**2012**). "Novel 1,2,4-triazolo[3,4-*b*]-1,3,4-thiadiazole derivatives as dual analgesic/anti-inflammatory and antimicrobial agents," Lett. Drug. Des. Discov. **9**, 204–212.

van de Streek, J. (**2015**). "Structure of Pigment Yellow 181 dimethylsulfoxide *N*-methyl-2-pyrrolidone (1:1:1) solvate from XRPD + DFT-D," Acta Crystallogr. B. **71**, 89–94.

van de Streek, J. and Neumann, M. A. (**2010**). "Validation of experimental molecular crystal structures with dispersion-corrected density functional theory calculations," Acta Crystallogr. B. **66**, 544–558.

van de Streek, J. and Neumann, M. A. (**2014**). "Validation of molecular crystal structures from powder diffraction data with dispersion-corrected density functional theory (DFT-D)," Acta Crystallogr. B. **70**, 1020–1032.

Wu, P. (**2013**). "Crystal structure of 6-ferrocenyl-3-phenyl-[1,2,4]triazolo[3,4-*b*][1,3,4]thiadiazole," J. Struct. Chem. **54**(5), 983–985.

https://doi.org/10.1017/S0885715619000654 Published online by Cambridge University Press